

CONFIDENTIAL

Copy
RM L55F06a

6

NACA RM L55F06a



NACA

RESEARCH MEMORANDUM

INVESTIGATION AT TRANSONIC SPEEDS OF THE HINGE-MOMENT

CHARACTERISTICS OF A 1/8-SCALE MODEL

OF THE X-1E AILERON

By William C. Moseley, Jr.

Langley Aeronautical Laboratory

Langley Field, Va.

CLASSIFICATION CHANGED

UNCLASSIFIED

To _____

By authority of *NASA TPA 9* *Effective*
Date *9-1-59*
NB 11-20-59 CLASSIFIED DOCUMENT

This material contains information affecting the National Defense of the United States within the meaning of the espionage laws, Title 18, U.S.C., Secs. 793 and 794, the transmission or revelation of which in any manner to an unauthorized person is prohibited by law.

NATIONAL ADVISORY COMMITTEE FOR AERONAUTICS

WASHINGTON

August 5, 1955

CONFIDENTIAL LABORATORY
RESEARCH REPORT
LANGLEY FIELD, VIRGINIA

CONFIDENTIAL

UNCLASSIFIED

UNCLASSIFIED

NATIONAL ADVISORY COMMITTEE FOR AERONAUTICS

RESEARCH MEMORANDUM

INVESTIGATION AT TRANSONIC SPEEDS OF THE HINGE-MOMENT

CHARACTERISTICS OF A 1/8-SCALE MODEL

OF THE X-1E AILERON

By William C. Moseley, Jr.

SUMMARY

An investigation was made in the Langley high-speed 7- by 10-foot tunnel to determine the transonic hinge-moment characteristics of a low-aspect-ratio wing with a flap-type control. The tests were made with a 1/8-scale model of the outboard 35 percent semispan of the X-1E research airplane wing. The model had an aspect ratio of 1.80; a taper ratio of 0.74, and a modified NACA 64A004 airfoil. The tests were made through an angle-of-attack range of -4° to 10° , an aileron-deflection range of at least $\pm 7^{\circ}$, and a Mach number range of 0.60 to 1.08. The Reynolds number based on the mean aerodynamic chord was approximately 2.0×10^6 .

The slopes of the curves of hinge-moment coefficient with angle of attack and control deflection were generally constant in the subsonic range up to a Mach number of 0.90. The negative values of the hinge-moment parameters decreased slightly between Mach numbers of 0.90 and 0.95, and above a Mach number of 0.95 there were rapid negative increases until the values at a Mach number of 1.08 were several times the subsonic values.

INTRODUCTION

Extensive research by the National Advisory Committee for Aeronautics has indicated that airfoil thickness is of primary importance in the performance of aircraft designed to operate in the transonic and supersonic speed ranges. As a result of these findings, a 4-percent-thick, aspect-ratio-4 wing is being installed on the Bell X-1 research airplane to further evaluate these findings. Low-speed investigations using a 1/4-scale model of the new airplane configuration have been made to determine the static stability and control characteristics, and pressure distributions across the slotted flap and aileron. (See refs. 1 and 2.)

UNCLASSIFIED

The purpose of the present investigation is to determine the aileron hinge-moment characteristics in the transonic speed range. The tests were made with a 1/8-scale model of the outboard 35-percent-semispan part of the X-1E research airplane wing. Because of differences in aspect ratio, taper ratio, and relative span of the aileron to wing span between the present wing and the full-scale wing, a question arises as to whether these aileron hinge-moment data will indicate what can be expected on the X-1E airplane. It is felt that these hinge-moment data will give a reliable indication of the trends expected on the full-scale airplane because the more important parameters which affect hinge moments such as overhang balance, seal, gap, and trailing-edge angle have been simulated on the model. The lift and rolling-moment data from the model tests are not indicative of what is expected of the complete model of the X-1E; however, they are included herein as a source of information.

The tests were made through a Mach number range of 0.60 to 1.08, an angle-of-attack range of -4° to 10° , and an aileron-deflection range between $\pm 7^\circ$ and $\pm 10^\circ$. The Reynolds number based on the mean aerodynamic chord varied with Mach number from about 1.70×10^6 to 2.15×10^6 .

SYMBOLS

C_h	aileron hinge-moment coefficient, $\frac{\text{Hinge moment of aileron about hinge line}}{2M'q}$
C_L	lift coefficient, $\frac{\text{Twice lift of semispan model}}{qS}$
C_l	rolling-moment coefficient at plane of symmetry, about stability x-axis, $\frac{\text{Rolling moment of semispan model}}{qSb}$
q	effective dynamic pressure over span of model, lb/sq ft
M'	area moment of aileron rearward of hinge line, 0.00412 ft ³
S	twice wing area of semispan model, 0.558 sq ft
b	twice span of semispan model, 0.997 ft
b_a	span of aileron, 0.427 ft

- \bar{c} mean aerodynamic chord, based on relationship $\frac{2}{S} \int_0^{b/2} c^2 dy$
(using theoretical tip), 0.564 ft
- c local wing chord, ft
- c_a aileron chord equal to 0.25c, ft
- c_b overhang-balance chord equal to 0.20c_a, ft
- y spanwise distance from reflection plane, ft
- M effective Mach number over span of model, $\frac{2}{S} \int_0^{b/2} c M_a dy$
- M_a average chordwise local Mach number
- M_l local Mach number
- A aspect ratio, b^2/S
- R Reynolds number of wing based on \bar{c}
- α angle of attack, deg
- δ aileron deflection, measured in a plane normal to hinge line,
positive when trailing edge is below wing-chord plane, deg

$$C_{L\alpha} = \left(\frac{\partial C_L}{\partial \alpha} \right)_{\delta}$$

$$C_{L\delta} = \left(\frac{\partial C_L}{\partial \delta} \right)_{\alpha}$$

$$C_{l\delta} = \left(\frac{\partial C_l}{\partial \delta} \right)_{\alpha}$$

$$c_{h\alpha} = \left(\frac{\partial c_h}{\partial \alpha} \right)_{\delta}$$

$$c_{h\delta} = \left(\frac{\partial c_h}{\partial \delta} \right)_{\alpha}$$

The subscript outside the parentheses indicates the factor held constant during the measurement of the parameters.

MODEL AND APPARATUS

The model used for this investigation, shown in figure 1, was a 1/8-scale model of the outboard 35 percent semispan of the X-1E wing and had an aspect ratio of 1.80, a taper ratio of 0.74, 0° sweepback of the 0.40-chord line, and a modified NACA 64A004 airfoil section. The part of the wing rearward of the 0.70-chord line had a straight-line fairing so that the trailing edge had a constant percentage thickness equal to 0.003cc which gave a trailing-edge angle of 4.1°. The forward part of the wing was constructed with a steel core and a plastic finished surface.

The 0.25c flap-type aileron extended from the 0.086b/2 model station to the 0.943b/2 model station, and had a 0.20c_a (0.05c) overhang balance which extended from the 0.171b/2 model station to the 0.943b/2 model station. The gap between the aileron and wing was 1/64 inch and was left unsealed for these tests. The aileron had a steel spar and a spruce trailing-edge part that was covered with silk. In order to minimize the possibility of coupled wing-aileron flutter, the flap was statically mass balanced by a tungsten insert in the steel overhang as shown in figure 1. The aileron was attached to the wing by simple bearing hinges at each end. The model was mounted on an electrical strain-gage balance system which was attached rigidly to the tunnel wall, and the lift and rolling moment were indicated by means of calibrated potentiometers. The hinge rod at the inboard end of the aileron extended below the reflection plane. To this rod a calibrated electrical strain gage was attached and was used to give an indication of the aileron hinge moments.

TESTS

The tests were made in the Langley high-speed 7- by 10-foot tunnel with the side-wall reflection-plane test setup. This technique involved

the mounting of the model in a high-velocity flow field over a reflection plate mounted near the tunnel side wall. (See ref. 3.)

Typical contours of the local Mach number in the vicinity of the model location obtained with no model in place are shown in figure 2. The effective test Mach numbers were obtained from similar contour charts with the relationship

$$M = \frac{2}{5} \int_0^{b/2} cM_a dy$$

The variation of Reynolds number based on a mean aerodynamic chord of 0.564 foot with Mach number is presented in figure 3. The width of the band in figure 3 represents the maximum variation of Reynolds number with changing atmospheric conditions.

Static measurements of lift, rolling moment, and aileron hinge moment were obtained through a Mach number range of 0.60 to 1.08, an angle of attack range of -4° to 10° , and a range of aileron deflections which varied from about $\pm 10^\circ$ at the low Mach numbers to about $\pm 7^\circ$ at the higher Mach numbers. The lift data represent the aerodynamic effects that would be obtained on a complete wing with both surfaces deflected in the same direction as full-span flaps.

CORRECTIONS

No corrections have been applied to the data for hinge friction, for the chordwise and spanwise velocity gradients, or for distortion of the model due to air load; but these corrections are believed to be small. Flap deflections have been corrected for twisting of the hinge rod of small diameter between the hinge-moment strain gage and the control. Flap-deflection corrections were determined from a static hinge-moment calibration and were applied according to the measured test hinge moment. This correction was large and for extreme loading conditions was about 40 percent of the original control setting. Despite the large corrections applied, the final deflections presented are believed to be reliable since care was taken not to exceed the proportional limit of the hinge rod. Aileron deflections presented are for the midspan of the aileron and are considered average deflections.

No reflection-plane corrections have been applied to the data for the rolling-moment coefficient as plotted against δ , but the parameter C_{l_δ} given in this paper has been reduced by a factor obtained from unpublished experimental data obtained at low speed ($M = 0.25$) and

theoretical considerations. Although the reductions are based on incompressible conditions and are only valid for low Mach numbers, they were applied throughout the Mach number range in order to give a better representation of the true conditions than would be shown by the uncorrected data. For the configuration of the present investigation, the correction was applied as follows:

$$C_{l\delta} = \left(C_{l\delta} \right)_{\text{measured}} - 0.13 \left(C_{l\delta} \right)_{\text{measured}}$$

The lift data represent the aerodynamic effects that would be obtained on a complete wing with both control surfaces deflected in the same direction and, therefore, no reflection-plane corrections are necessary.

RESULTS AND DISCUSSION

As pointed out previously in this paper, the model used in this investigation was a 1/8-scale model of only the outboard 35 percent semispan of the X-1E wing. Although this presents an immediate problem as to the direct applicability of the data to the X-1E airplane, it is felt that because the airfoil section is the same as that of the X-1E airplane the trends of the hinge-moment parameters and the variation with Mach number should be similar to those for a complete semispan model. Lift- and rolling-moment-coefficient data have also been included as a source of information. Because of large differences in $\frac{b_a}{b/2}$, aspect ratio, and taper ratio, the lift and rolling-moment data would be quite different from those obtained on a model of the complete semispan; however, these parameters are felt to have only a minor effect on the magnitudes and variations of hinge moment.

The data are presented in the following figures:

	Figure
Variation of lift, rolling-moment, and hinge-moment coefficients with aileron deflection for various angles of attack and Mach numbers	4
Variation of hinge-moment parameters with Mach number	5
Variation of lift and rolling-moment parameters with Mach number	6

Hinge Moment

The hinge-moment-coefficient data in figure 4 show that the variation of hinge-moment coefficient with aileron deflection was linear only over a small deflection range near zero deflection, with large increases in hinge moment at the higher deflection angles. The hinge-moment-parameter data (fig. 5) show very little variation in $C_{h\delta}$ with Mach number up to about $M = 0.95$ where an abrupt negative increase in $C_{h\delta}$ occurred; at $M = 1.08$ the negative value of $C_{h\delta}$ was about four times as large as the value at $M = 0.95$. The variation of $C_{h\alpha}$ with Mach number was small up to $M = 0.90$. Between $M = 0.90$ and 1.0 there was a slight negative decrease in $C_{h\alpha}$, whereas above $M = 1.0$ a sharp negative increase in $C_{h\alpha}$ occurred. These trends in hinge-moment-parameter variation with Mach number are very similar to variations obtained with swept-wing configurations, that is, almost constant at the lower Mach numbers with an abrupt negative increase in the vicinity of $M = 0.95$ until sonic or low supersonic values are several times the low subsonic values. (See refs. 4, 5, and 6.)

The subsonic values of $C_{h\alpha}$ and $C_{h\delta}$ obtained were approximately -0.0025 and -0.0067 , respectively. These values compare favorably with the values of -0.0038 and -0.0083 obtained in the low-speed tests of reference 1. The aileron of reference 1 had a slightly thicker trailing edge than the present model; this difference could partially account for the slightly higher negative values of $C_{h\alpha}$ and $C_{h\delta}$. (See ref. 4.) Estimates for the ailerons on the wing with aspect ratio 4, based on the charts of reference 7 which were determined from low-speed investigations, indicate that $C_{h\alpha}$ and $C_{h\delta}$ would be -0.0035 and -0.0090 , respectively.

Lift and Rolling Moment

The lift-coefficient data in figure 4 show that the aileron was effective in producing lift throughout the Mach number range up to the maximum Mach number of $M = 1.08$ where a loss of effectiveness for some angles of attack occurred at the higher aileron deflections. As can be noted in figure 6, the lift parameter $C_{L\delta}$ was generally constant with Mach number up to $M = 0.95$. At $M = 0.95$ an abrupt decrease in $C_{L\delta}$ occurred until the maximum test Mach number was obtained. The value of $C_{L\delta}$ at $M = 1.08$ was approximately 40 percent of the value

at $M = 0.95$. The lift-curve slope C_{L_α} as shown in figure 6 increased as Mach number was increased up to about $M = 1.0$ where a slight decrease in C_{L_α} occurred. An estimation of the lift-curve slope based on the data of reference 8 gives a value of 0.040 which compares with a value of 0.042 at $M = 0.6$.

The rolling-moment coefficient data of figure 4 show a variation with deflection and Mach number very similar to the lift coefficient data. The aileron-effectiveness parameter C_{l_δ} was generally constant with increase in Mach number up to $M = 0.95$. Above $M = 0.95$, as the Mach number was increased, C_{l_δ} decreased until the value of C_{l_δ} at $M = 1.08$ was about 50 percent of the value at $M = 0.95$.

CONCLUDING REMARKS

An investigation was made in the Langley high-speed 7- by 10-foot tunnel to determine the transonic hinge-moment characteristics of the aileron of the X-1E research airplane. The variations of the hinge-moment parameters C_{h_α} and C_{h_δ} with Mach number were very similar to those experienced on swept-wing configurations; that is, large negative increases between Mach numbers 0.95 and 1.00 until at a Mach number of 1.00 the values of C_{h_α} and C_{h_δ} were several times the subsonic values.

Langley Aeronautical Laboratory,
National Advisory Committee for Aeronautics,
Langley Field, Va., May 25, 1955.

REFERENCES

1. Moseley, William C., Jr., and Taylor, Robert T.: Low-Speed Static Stability and Control Characteristics of a $1/4$ -Scale Model of the Bell X-1 Airplane Equipped With a 4-Percent-Thick, Aspect-Ratio-4, Unswept Wing. NACA RM L53H27, 1953.
2. Moseley, William C., Jr., and Taylor, Robert T.: Low-Speed Chordwise Pressure Distributions Near the Midspan Station of the Slotted Flap and Aileron of a $1/4$ -Scale Model of the Bell X-1 Airplane With a 4-Percent-Thick, Aspect-Ratio-4, Unswept Wing. NACA RM L53L18, 1954.
3. Donlan, Charles J., Myers, Boyd C., II, and Mattson, Axel T.: A Comparison of the Aerodynamic Characteristics at Transonic Speeds of Four Wing-Fuselage Configurations As Determined From Different Test Techniques. NACA RM L50H02, 1950.
4. Thompson, Robert F.: Investigation of a 42.7° Sweptback Wing Model To Determine the Effects of Trailing-Edge Thickness on the Aileron Hinge-Moment and Flutter Characteristics at Transonic Speeds. NACA RM L50J06, 1950.
5. Thompson, Robert F., and Moseley, William C., Jr.: Hinge-Moment and Control-Effectiveness Characteristics of an Outboard Flap With an Overhang Nose Balance on a Tapered 35° Sweptback Wing of Aspect Ratio 4. Transonic-Bump Method. NACA RM L52G08, 1952.
6. Johnson, Harold I.: Measurements of Aerodynamic Characteristics at Transonic Speeds of an Unswept and Untapered NACA 65-009 Airfoil Model of Aspect Ratio 3 With $1/4$ -Chord Plain Flap by the NACA Wing-Flow Method. NACA RM L53D21, 1953.
7. Langley Research Staff (Compiled by Thomas A. Toll): Summary of Lateral-Control Research. NACA Rep. 868, 1947. (Supersedes NACA TN 1245.)
8. DeYoung, John, and Harper, Charles W.: Theoretical Symmetric Span Loading at Subsonic Speeds for Wings Having Arbitrary Plan Form. NACA Rep. 921, 1948.

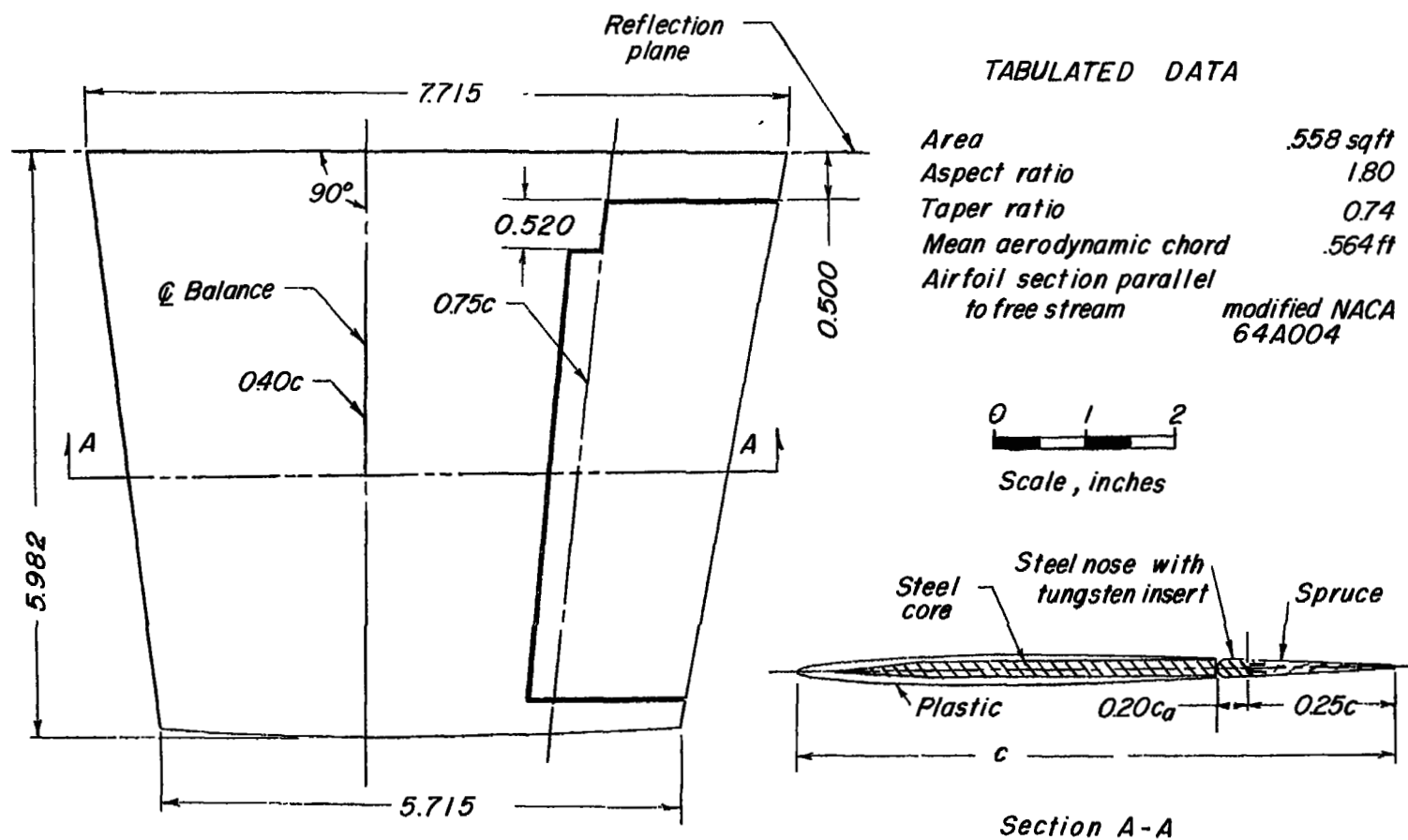


Figure 1.- General dimensions of the test model.

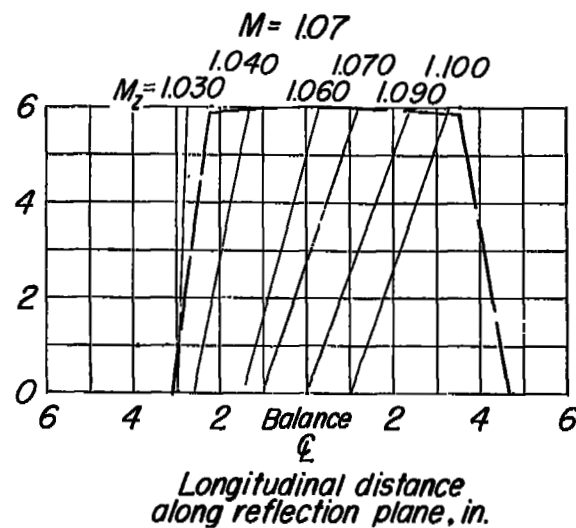
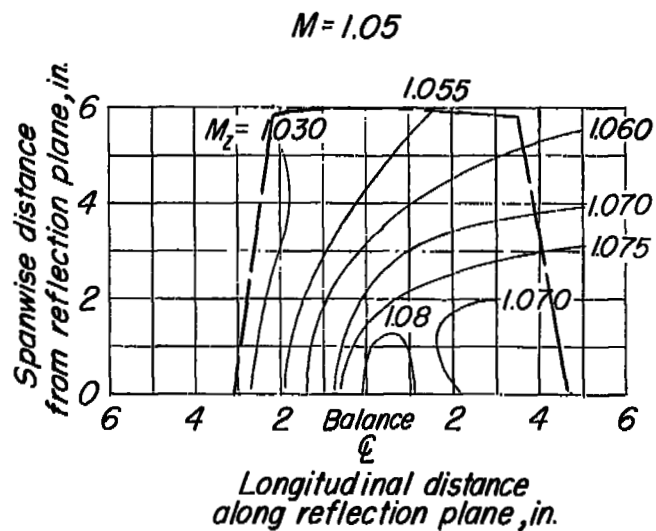
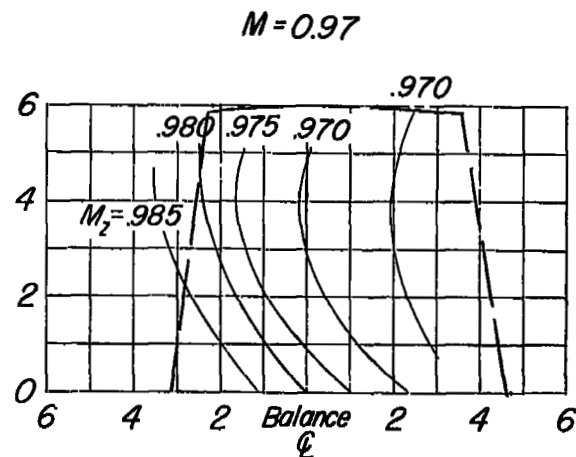
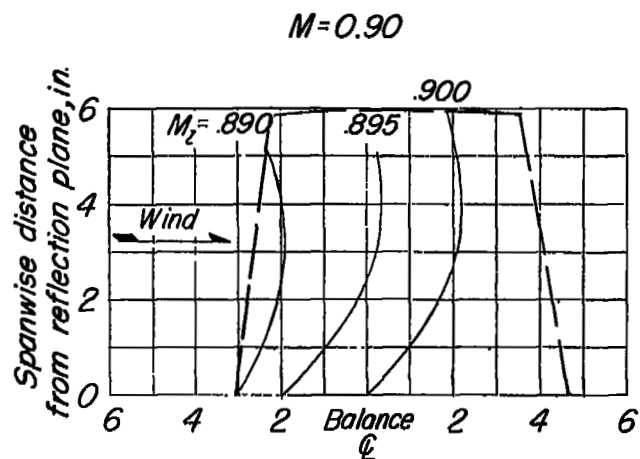


Figure 2.- Typical Mach number contours over the side-wall reflection plane.

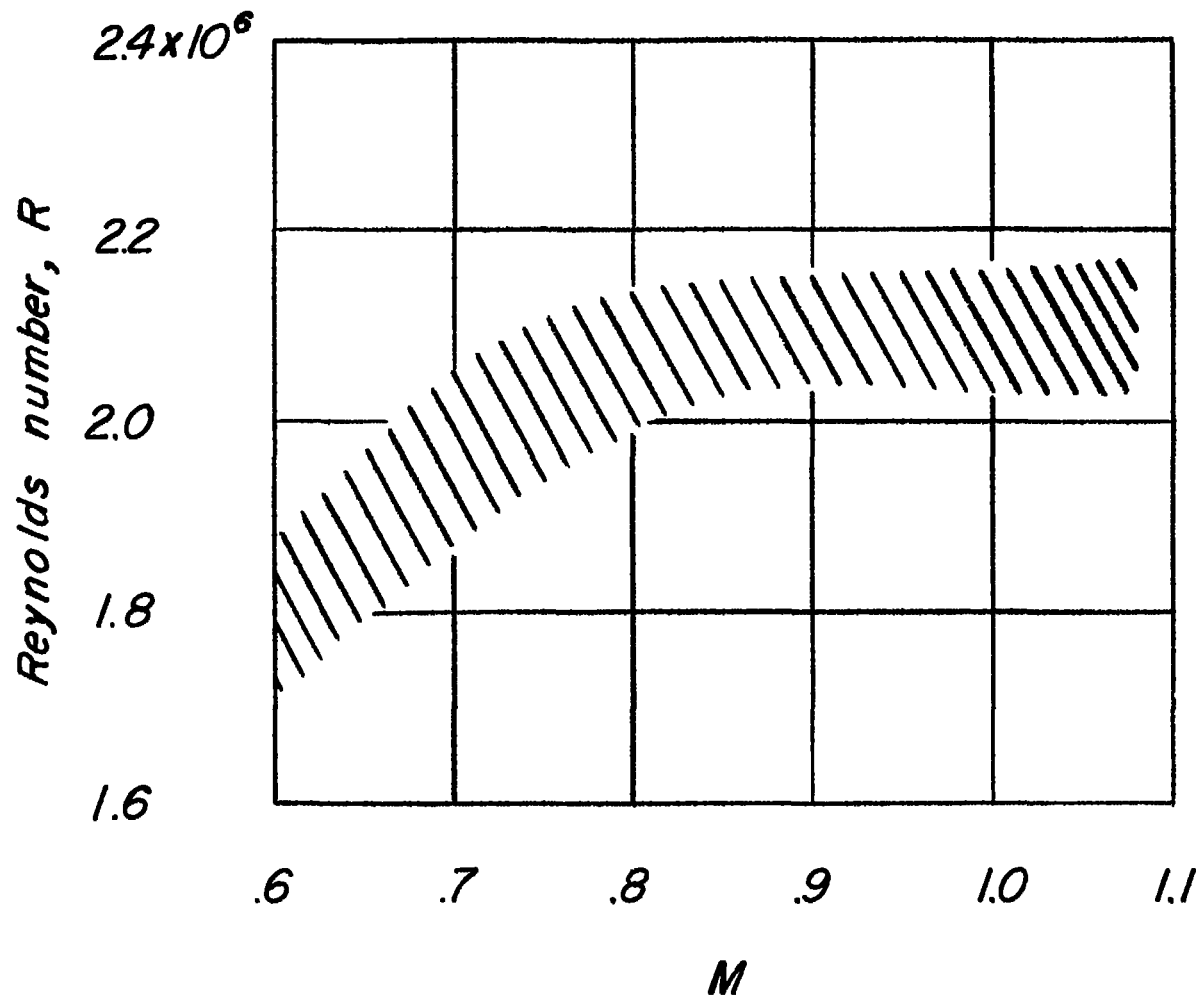
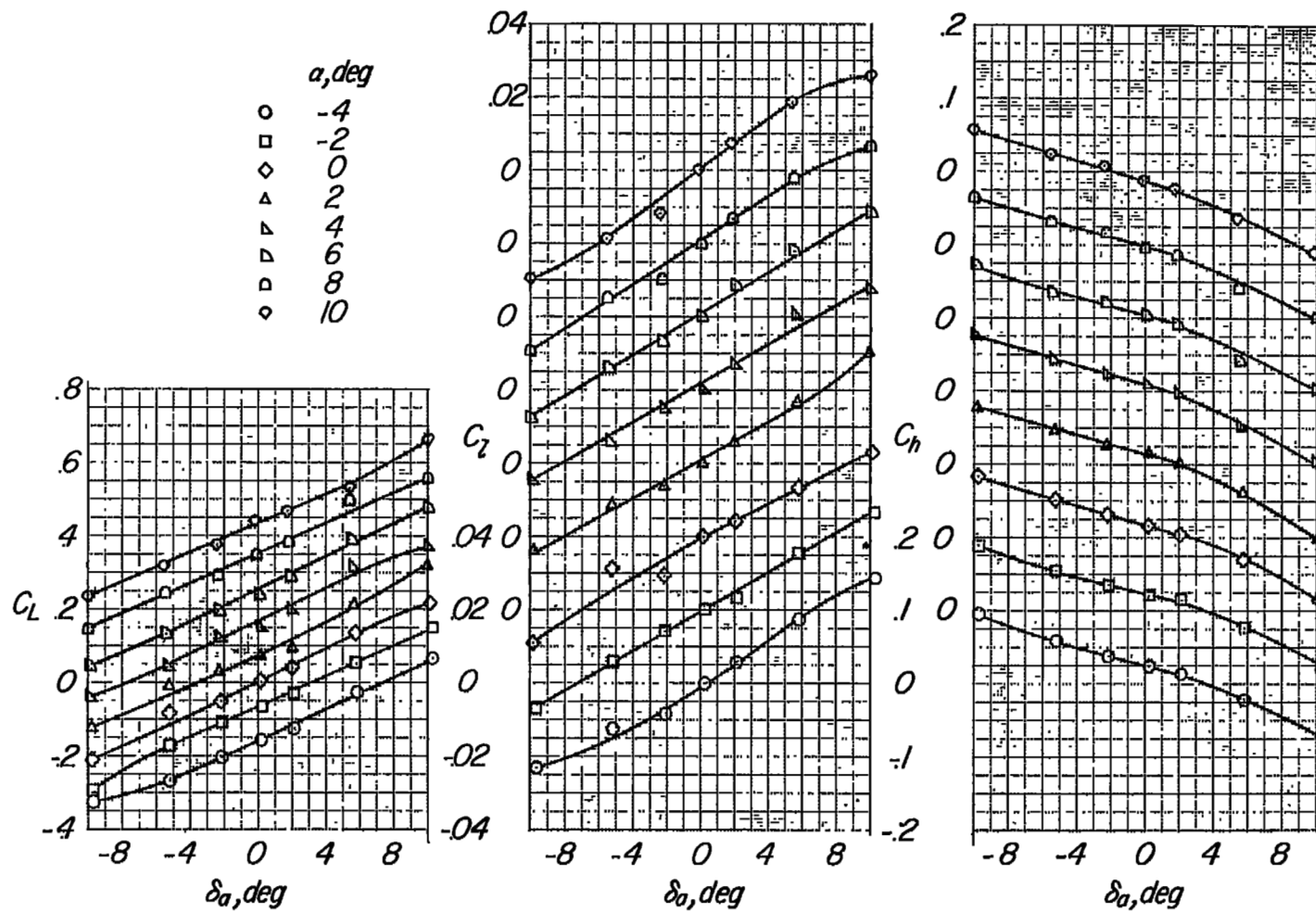
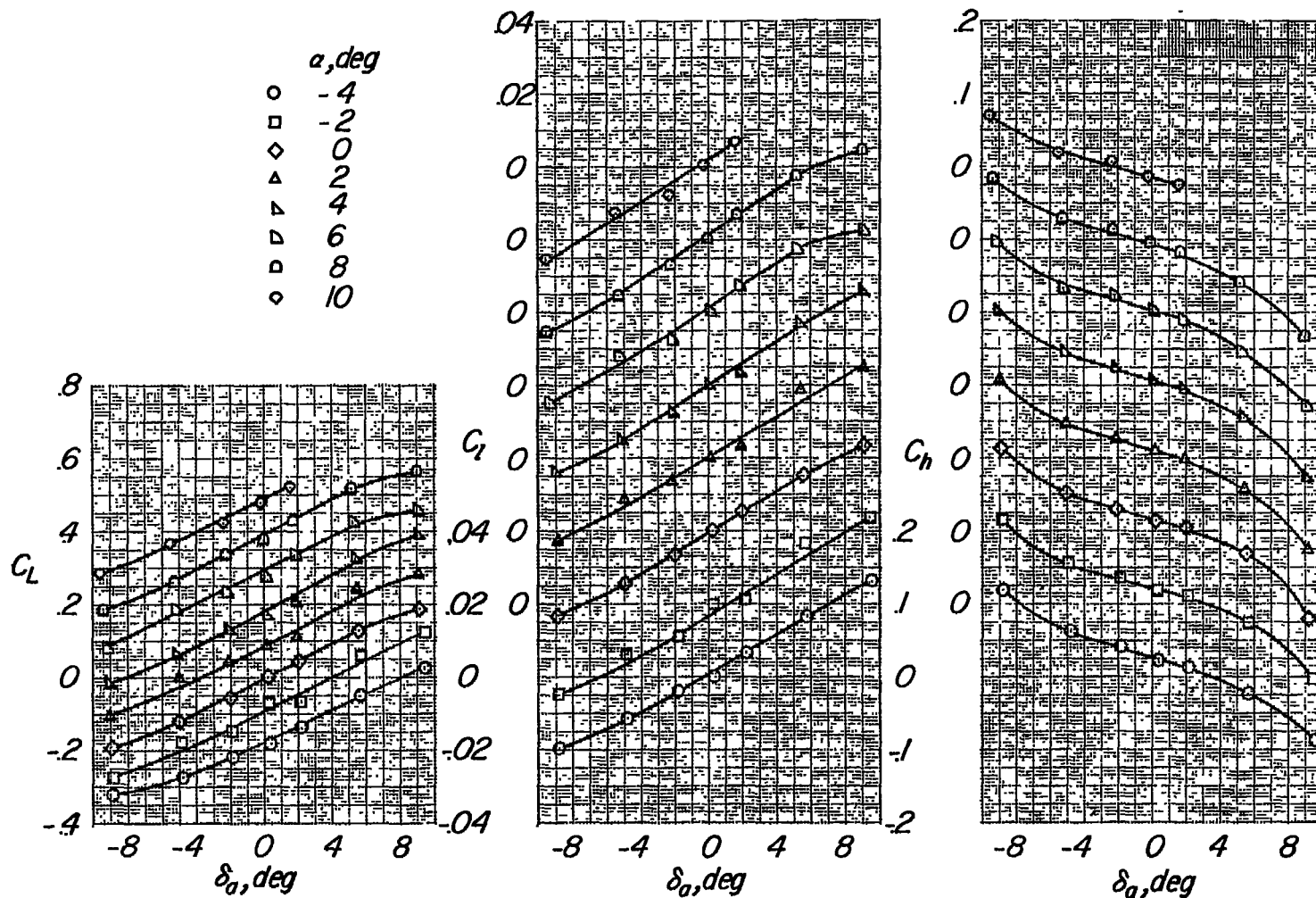


Figure 3.- Variation of Reynolds number with Mach number through the transonic speed range.



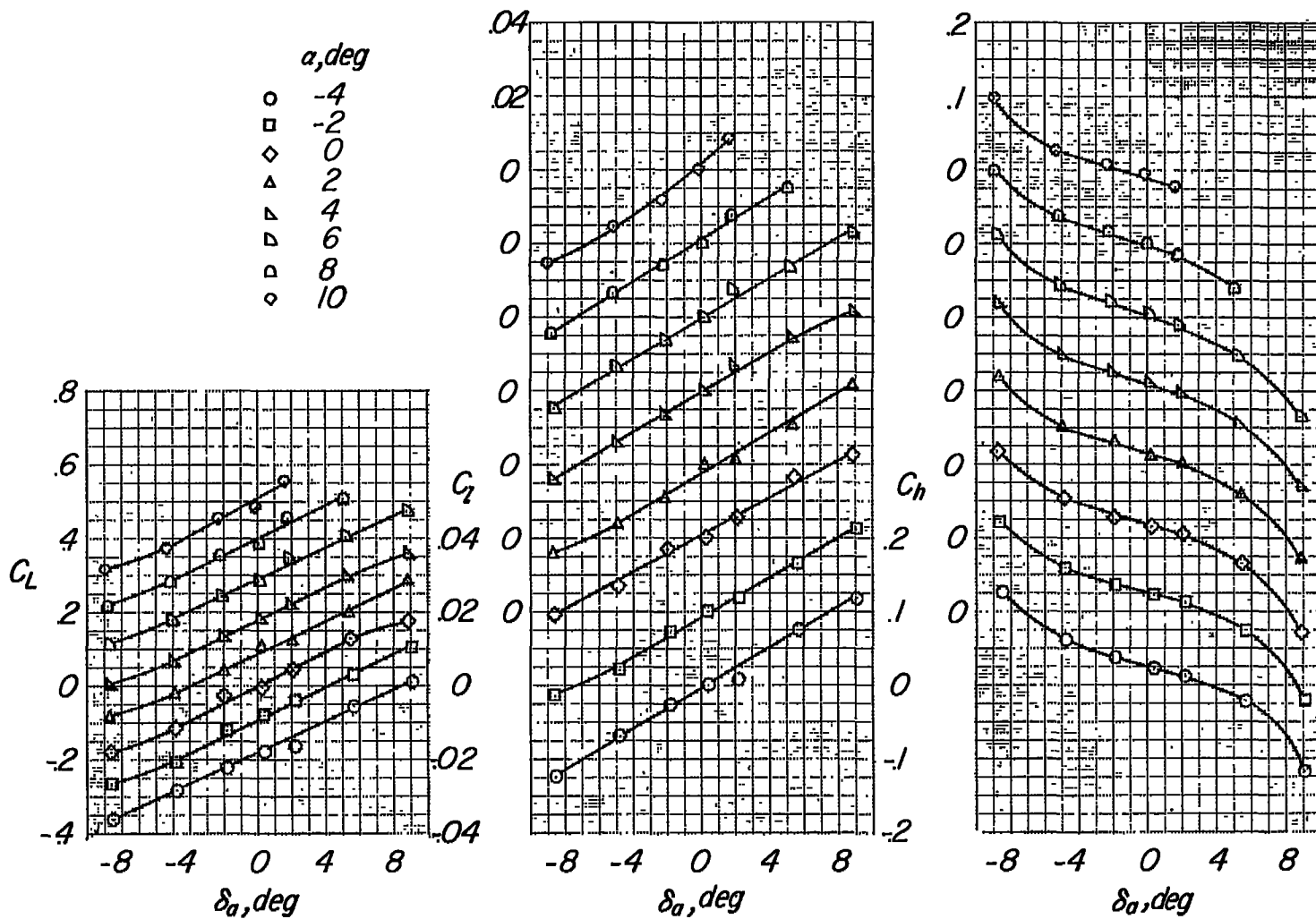
(a) $M = 0.60$.

Figure 4.- Variation of lift, rolling-moment, and hinge-moment coefficients with aileron deflection for various angles of attack and Mach numbers.



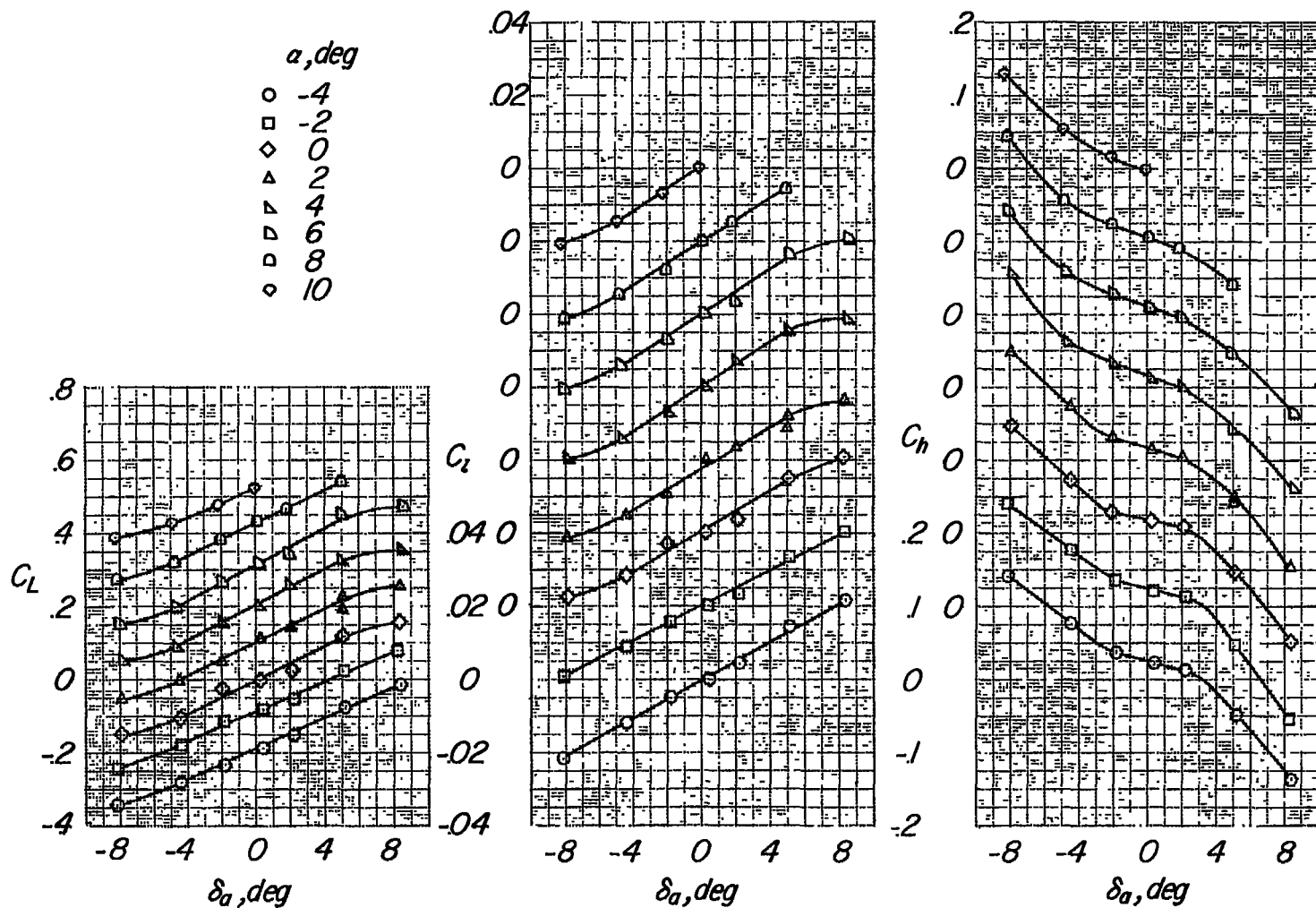
(b) $M = 0.80$.

Figure 4.- Continued.



(c) $M = 0.85$.

Figure 4.- Continued.



(d) $M = 0.90$.

Figure 4.- Continued.

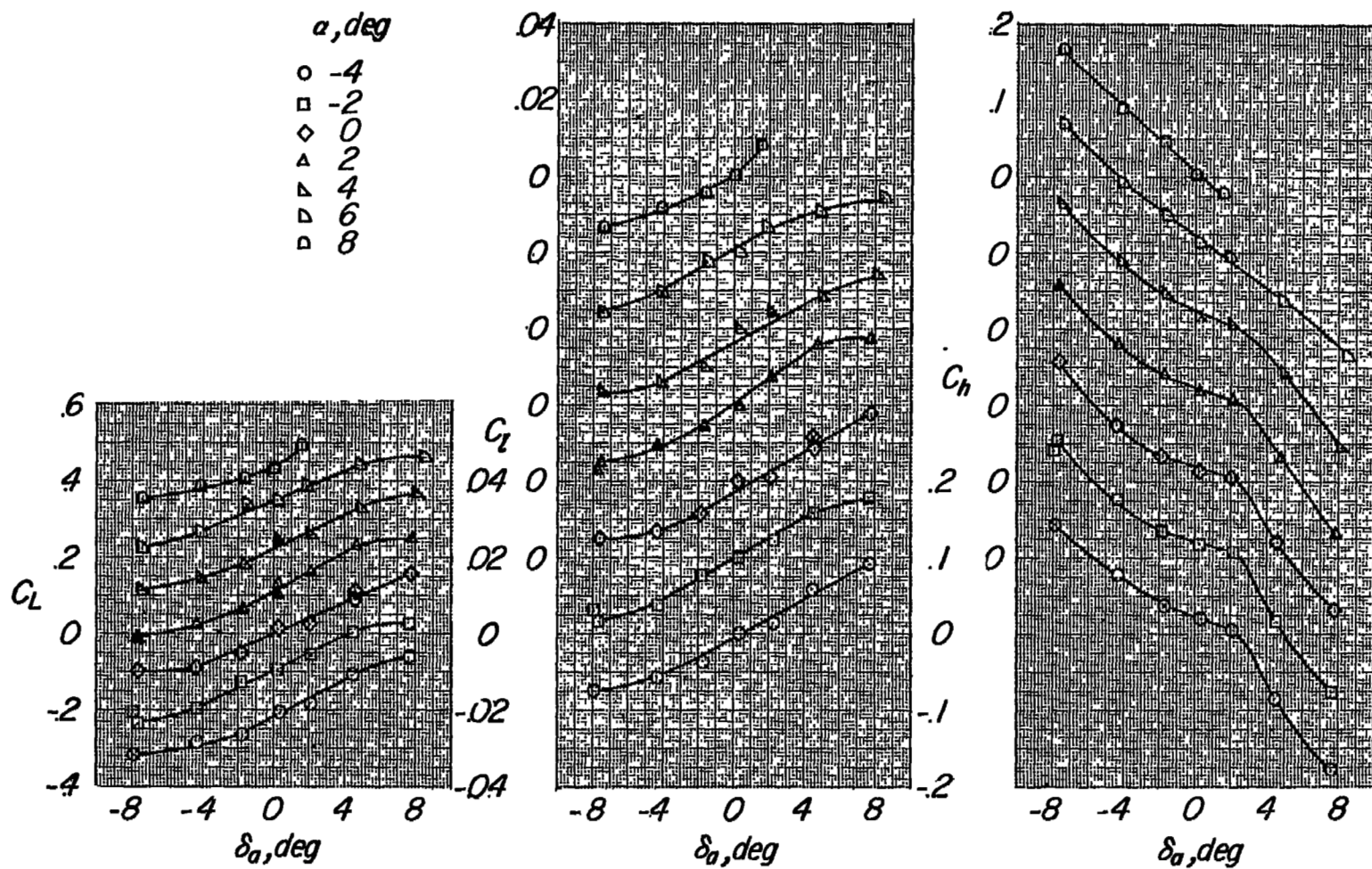
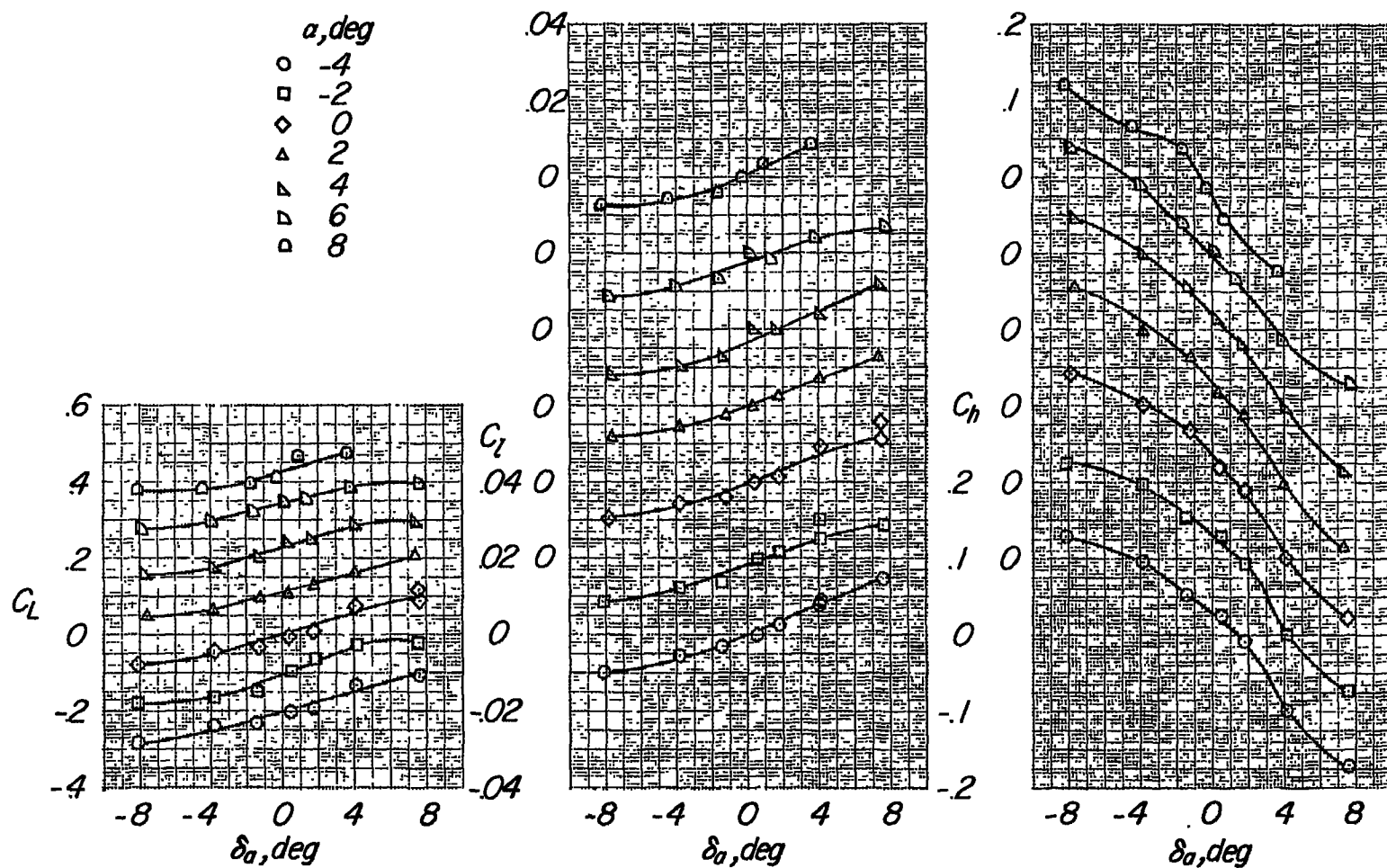
(e) $M = 0.95$.

Figure 4.- Continued.



(f) $M = 1.00$.

Figure 4.- Continued.

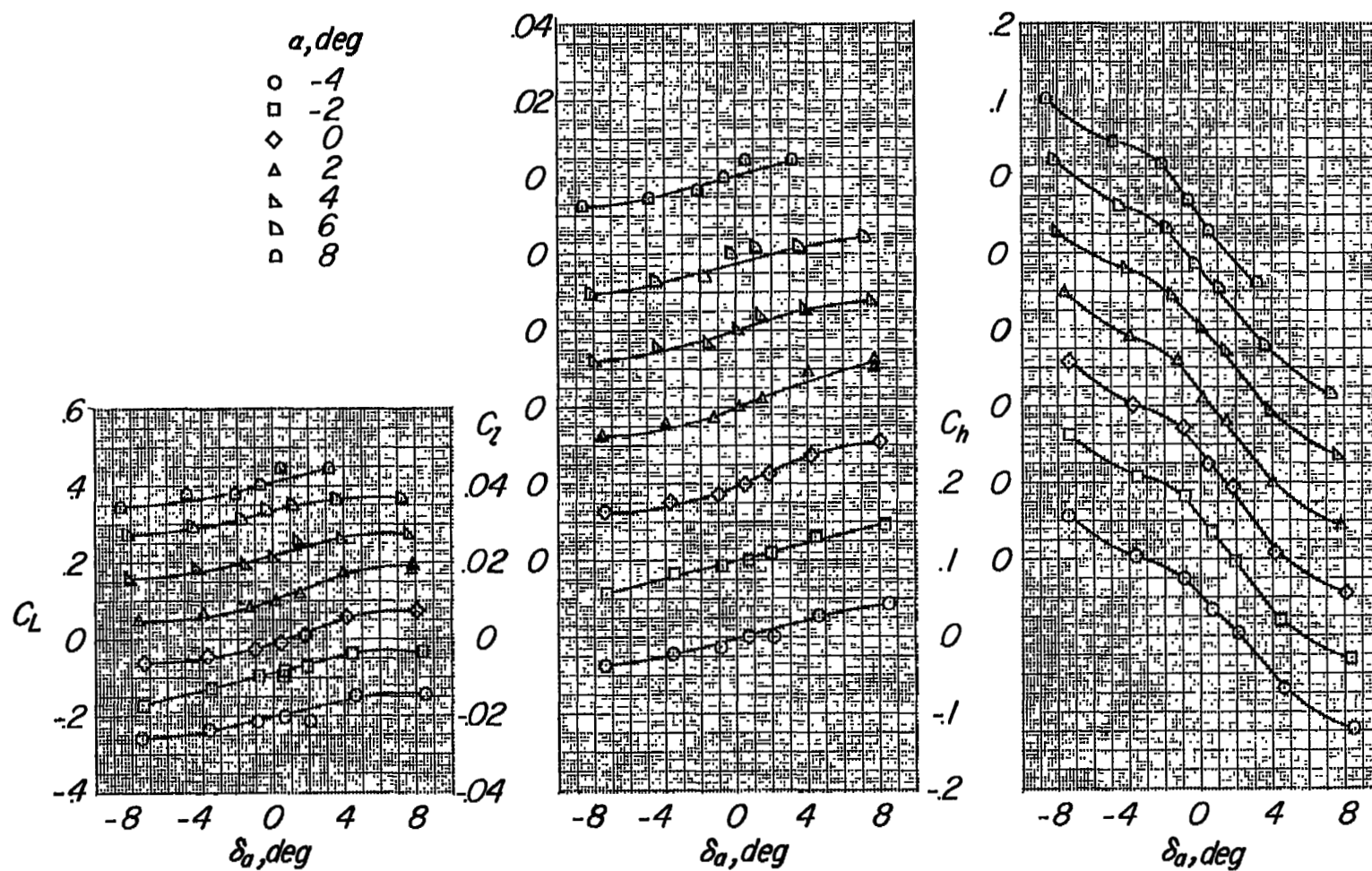
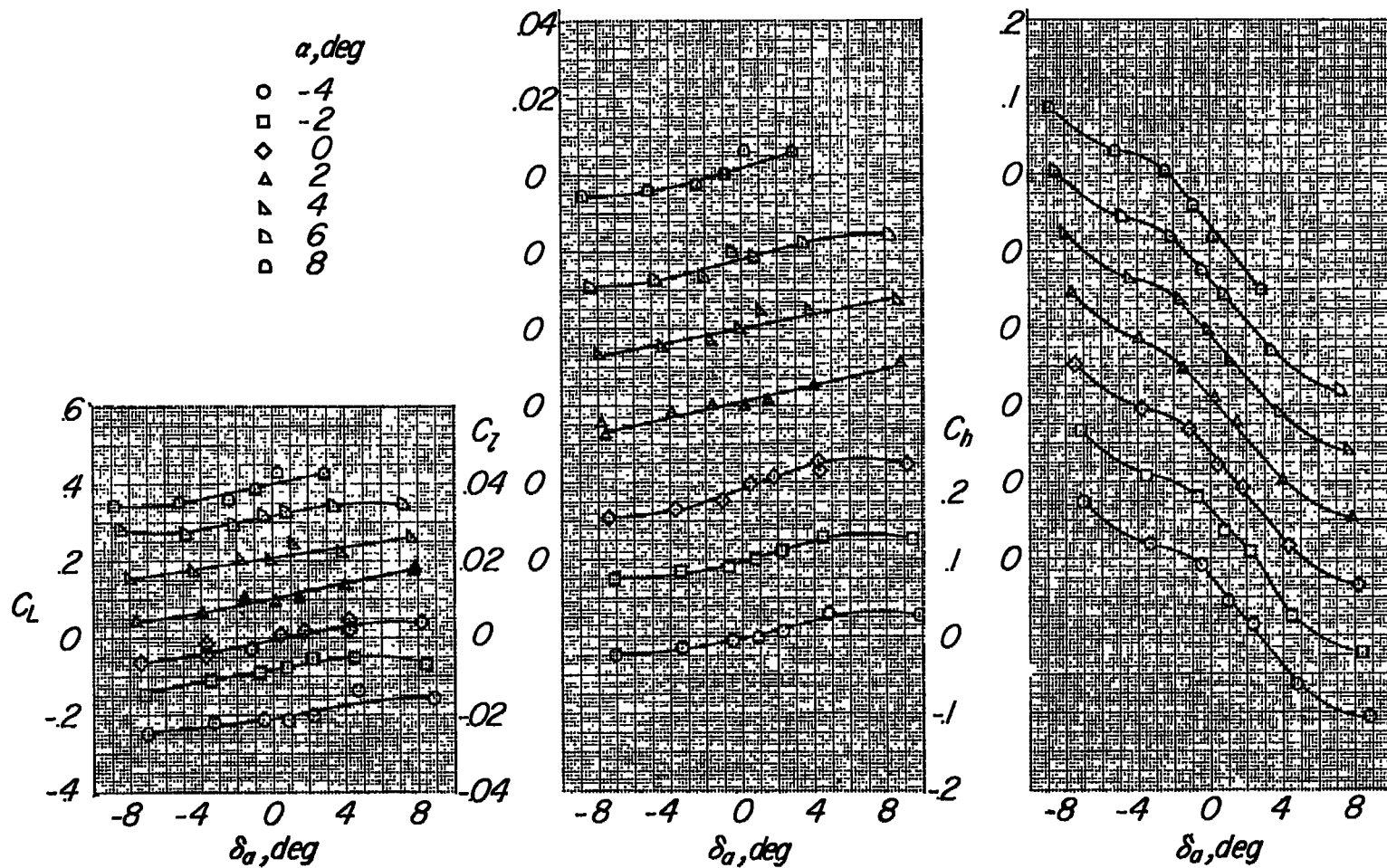
(g) $M = 1.05$.

Figure 4.- Continued.



(h) $M = 1.08$.

Figure 4.- Concluded.

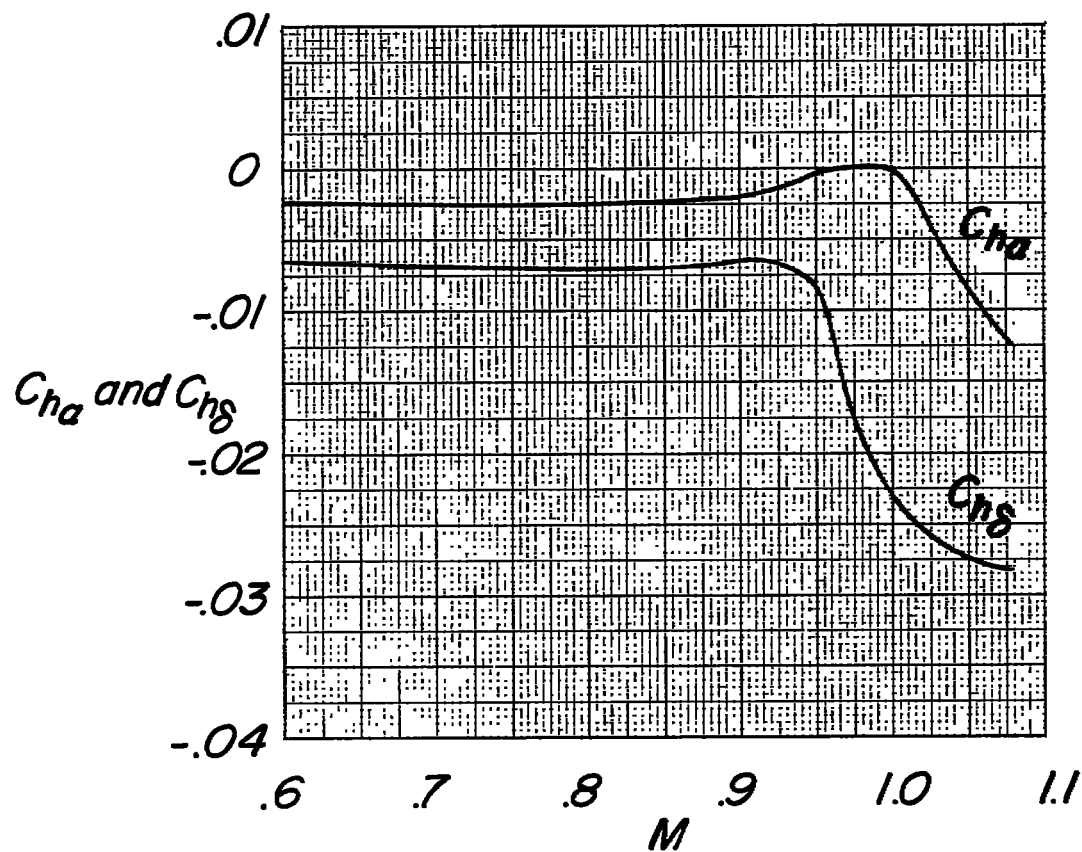


Figure 5.- Variation of the parameters $C_{h\alpha}$ and $C_{h\delta}$ with Mach number.

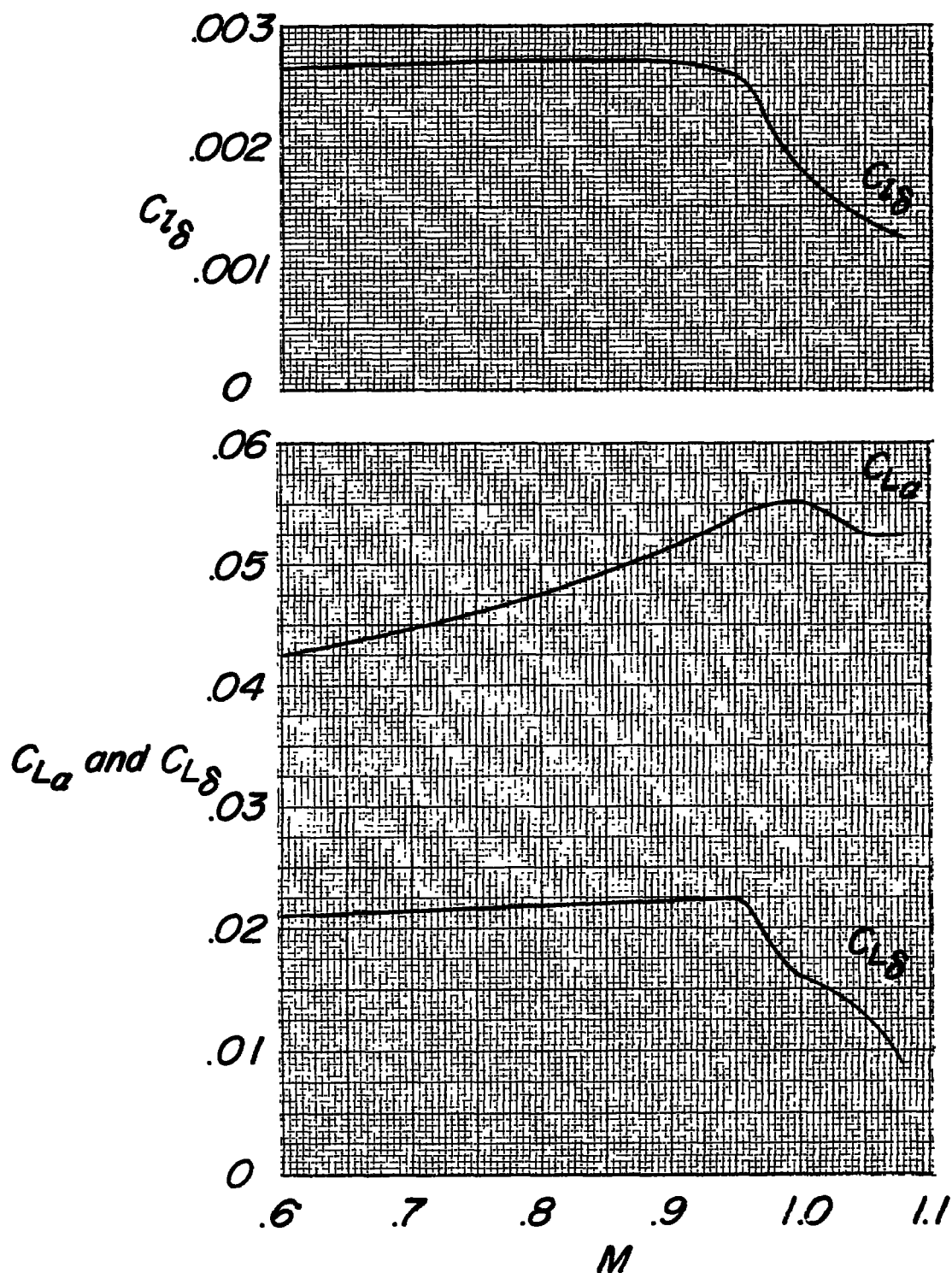


Figure 6.- Variation of the parameters $C_{L\delta}$, $C_{L\alpha}$, and $C_{L\delta}$ with Mach number.